Available online at www.sciencedirect.com

ScienceDirect

Current Opinion in Structural Biology

Serial femtosecond crystallography approaches to understanding catalysis in iron enzymes

Jonathan A. R. Worrall[1] and Michael A. Hough[1,2]

Abstract

Enzymes with iron-containing active sites play crucial roles in catalysing a myriad of oxidative reactions essential to aerobic life. Defining the three-dimensional structures of iron enzymes in resting, oxy-bound intermediate and substrate-bound states is particularly challenging, not least because of the extreme susceptibility of the Fe(III) and Fe(IV) redox states to radiation-induced chemistry caused by intense X-ray or electron beams. The availability of novel sources such as X-ray free electron lasers has enabled structures that are effectively free of the effects of radiation-induced chemistry and allows time-resolved structures to be determined. Important to both applications is the ability to obtain *in crystallo* spectroscopic data to identify the redox state of the iron in any particular structure or timepoint.

Addresses

[1] School of Life Sciences, University of Essex, Wivenhoe Park, Colchester, Essex CO4 3SQ, UK

[2] Diamond Light Source Ltd, Harwell Science and Innovation Campus, Didcot, Oxfordshire OX11 0DE, UK

Corresponding author: Hough, Michael A. (michael.hough@diamond.ac.uk)

Current Opinion in Structural Biology 2022, **77**:102486

This review comes from a themed issue on **Catalysis and Regulation (2022)**

Edited by **Danica Fujimori** and **Nigel Scrutton**

For a complete overview see the Issue and the Editorial

Available online xxx

https://doi.org/10.1016/j.sbi.2022.102486

Introduction

Metalloproteins-containing iron (Fe) carry out a tremendous variety of biological processes and have been a focus of attention since the earliest days of structural biology, with the pioneering X-ray crystal structures of myoglobin and hemoglobin [1,2]. Structural biology of Fe enzymes has subsequently revealed that nature employs a variety of protein scaffolds and Fe coordination geometries to harness the oxidative potential required for catalysis. The most prevalent Fe-containing enzymes that are utilised in aerobic biology possess active sites containing, heme, non-heme iron and non-heme diiron (Figure 1a). In each case, an Fe coordination site is available for binding of O_2 and/or H_2O_2 (Figure 1a), leading to the formation of reactive Fe-oxygen intermediates, including superoxo, hydroperoxo and high-valent Fe(IV)-oxo species (Figure 1b) that act as the basis for various biological functions [3–5].

Despite decades of advances in structural biology methodologies, considerable challenges remain in obtaining accurate and validated redox state structures of Fe-containing proteins. This is in part due to the high susceptibility of the metal centres to the ionising effects of the X-ray beam upon the crystals used for structure determination [6]. Redox states accessed by Fe enzymes are typically Fe(II), Fe(III) and Fe(IV) with the latter two being particularly prone to reduction by solvated electrons generated within the crystals by the X-ray beam [6,7]. This damage typically occurs far more rapidly with accumulated dose than is the case for more general radiation damage to the crystals resulting in unit cell expansion and loss of diffracting power [8]. Responding to this challenge, several adapted or novel methods have been developed to obtain intact and validated three-dimensional structures of Fe-containing proteins. In particular, the last decade has witnessed serial femtosecond crystallography (SFX) using X-ray free electron lasers (XFEL) that have transformed our ability to obtain intact and time-resolved structures [9–11].

Overview of SFX and complementary methodologies for the study of Fe-containing enzymes

Within the broad definition of SFX are several different methodologies and experimental approaches relevant to the study of Fe enzymes. SFX incurs a very high X-ray dose but with very short (a few tens of fs) pulses can produce structures where the electron density maps and related structures are essentially free of manifestations of X-ray induced chemistry [50]. Room temperature SFX structures can be obtained by measuring data from microcrystals in stable or semi-stable states, using multiple sample delivery methods [12,13], a detailed description of which is beyond the scope of this review but includes jets, extruders, fixed targets and droplets-on-tape based systems [9,14]. An alternative approach

Figure 1

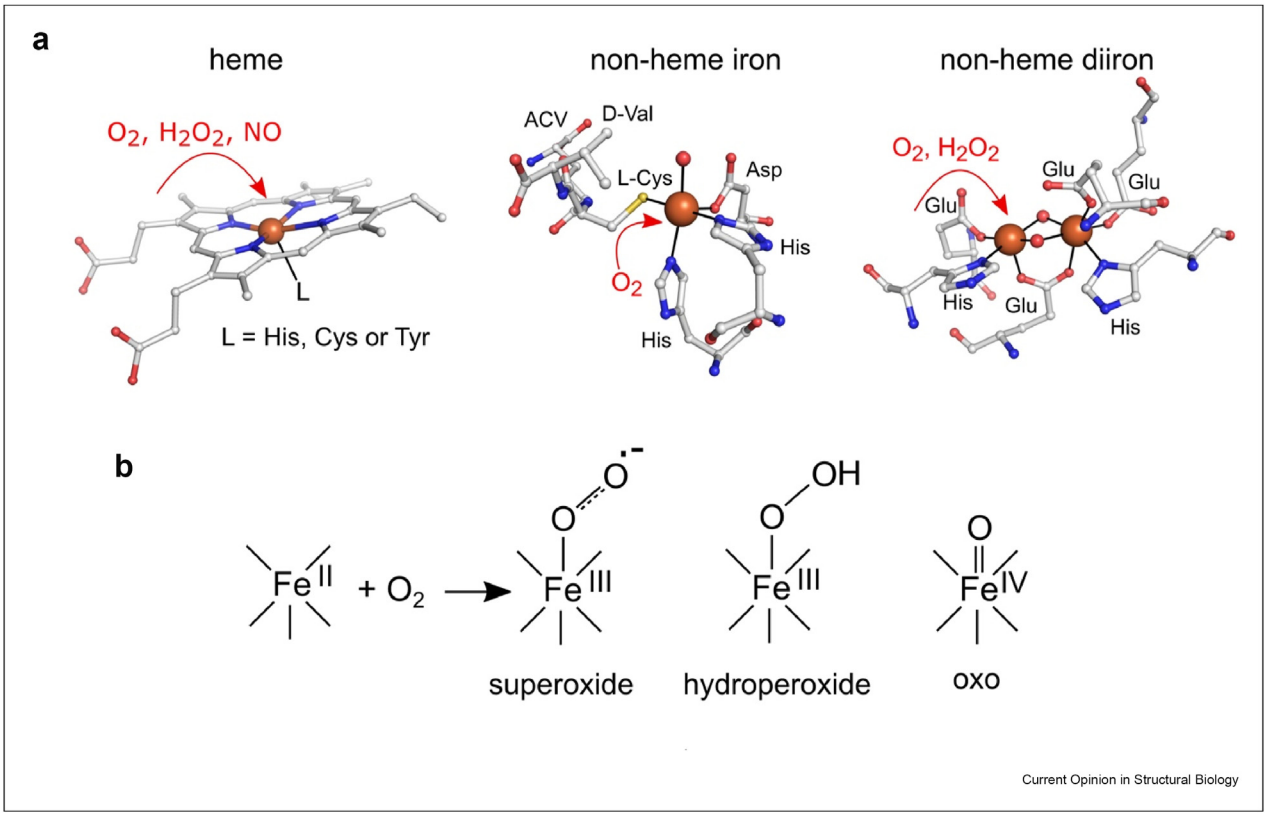

Examples of Fe coordinating active sites found in enzymes. **(a)** Heme (left panel) is found in peroxidases, catalases and cytochrome P450 members. The distal side of the heme-Fe is available for coordination of O_2 or H_2O_2, and in the case of P450 nitric oxide reductase (P450nor), NO [37]. Non-heme iron sites (centre panel) utilise His, carboxylate and H_2O (red sphere) as ligands, and in addition to binding O_2, can directly coordinate a substrate. Shown here is the ferrous site of isopenicillin *N* synthase (IPNS) from *Aspergillus nidulans*, a member of the 2-oxoglutarate oxygenase superfamily, with the linear tripeptide *d*-(L-α-aminoadipoyl)-L-cysteinyl-D-valine) (ACV) substrate bound (PDB code: 6ZAE) [44]. Non-heme diiron sites (right panel) also utilise His and carboxylate ligands with H_2O or hydroxide groups (red spheres) bridging the diiron centres. Shown here is the diferric site of soluble methane monooxygenase hydroxylase (sMMOH) from *Methylosinus trichosporium* OB3b [48]. Other examples include the ferroxidase centre of ferritins, with *Escherichia coli* bacterioferritin able to utilize H_2O_2 to oxidise the ferroxidase centre [49]. **(b)** The chemical nature of the different types of reactive iron-oxygen intermediates that can form in Fe enzymes upon activation of molecular oxygen.

is to cryo-cool either microcrystals on meshes or large single crystals that are then rotated, with the latter referred to as Serial Femtosecond Rotation Crystallography (SF-ROX) [15–17]. This can be useful in cryo-trapping intermediate species and in some cases has led to very high-resolution structures due to the larger crystal volume interacting with the XFEL beam [18]. In certain experimental arrangements, complementary spectroscopic data may be measured alongside diffraction or the microcrystal slurry may be characterised in bulk prior to beginning the experiment [17,19].

A long-standing approach to entirely avoid radiation-induced changes to active sites of Fe proteins is to use neutron diffraction (NX), which also has the great advantage that hydrogen atoms can be effectively resolved allowing information on protonation states of key amino acid residues and ligands to be explicitly identified [20]. However, NX requires very large crystals and lengthy data collection times often of many days and so its use has been limited to a comparatively small number of cases and it is also less amenable to time-resolved approaches [21]. One additional approach worthy of mention is to use conventional oscillation crystallography at synchrotron sources to produce small partial datasets from many crystals, consequently with very low associated X-ray doses. Single crystal spectroscopy is used prior to and following X-ray data collection to ensure that only minor radiation-induced changes have occurred and that the resulting composite structure is of a 'near to intact' redox state [22].

Recent detailed work from Srinivas et al. [23] applied a combination of X-ray emission spectroscopy (XES) and room temperature SFX to examine the non-heme diiron centre in soluble methane monooxygenase hydroxylase (sMMOH), that is able to convert the greenhouse gas methane to the fuel methanol [24]. SFX structures of

sMMOH in the diferric and diferrous forms in complex with the regulatory component, MMOB, were determined to 1.95 Å resolution [23]*. The complex structures revealed that on binding MMOB, the sMMOH diiron cavity undergoes a rearrangement, becoming more hydrophobic and thus increasing the affinity for the hydrophobic O_2 and methane molecules. Crucially, Fe Kα XES confirmed the Fe oxidation states in the complex, and corroborated that the shift in position of an active site Glu residue to replace one of the bridging hydroxo/aquo ligands (Figure 1) is due to the formation of the diferrous (active) state. These reorganisations offer new insight into how the complex enhances O_2 activation and methane oxidation [23].

XFEL structures of heme peroxidases in defined redox states

Peroxidases use high-valent Fe(IV) heme species (commonly known as ferryl) to carry out a wide range of one-electron oxidation chemistries [25]. A significant challenge for understanding molecular mechanisms of catalysis in heme peroxidases has been the high susceptibility of the ferryl intermediates, Compound I and Compound II, to reduction in the X-ray beam, which together with the often short-lived nature of these intermediates requires careful cryo-trapping of the appropriate enzyme state within crystals. Approaches to address this have included merging many low-dose multicrystal datasets together with validation of the electronic states using single crystal microspectrophotometry (thus obtaining close-to-intact structures) or NX which does not cause damage because the neutrons are scattered by nuclei rather than electrons [26–29]. A further challenge has been that protonation states of active site residues and the oxo adduct are important to understand for mechanism but are typically only identifiable in extremely high-resolution synchrotron data (often associated with high absorbed dose) or via NX [30].

The chemical nature of the ferryl species, Compound I and Compound II, in peroxidases has long been an intensive area of investigation, owing to the fact that the chemical nature i.e. Fe(IV)=O or Fe(IV)–OH is important for understanding reactivity and function. Several earlier, composite X-ray structures of cryo-trapped ferryl species have been reported [27,28] as well as a cryo-trapped XFEL structure of yeast cytochrome *c* peroxidase (CcP) [31]. Lucic et al. [29] applied room temperature SFX approaches using the dye type peroxidase DtpB from *Streptomyces lividans* which forms an unusually stable Compound I intermediate with a lifetime of several hours. An SFX structure of this ferryl intermediate after reaction initiation in bulk microcrystals by hydrogen peroxide was followed by immediate loading into a fixed target system for data collection at the SACLA XFEL. The resulting room temperature structure determined to 1.75 Å resolution reveals a short Fe–O bond (1.65 Å) that is consistent with a Fe(IV)=O species (Figure 2), and in line with Fe(IV)=O bond lengths determined under cryo-cooled conditions [32]. Interestingly, variability in the Fe–O bond length exists amongst the six protomers that make up the DtpB hexamer assembly. The mechanistic consequences for this variation on the oxidative potential of the ferryl species are at present unknown, but the observation supports the possibility that flexibility in Fe(IV)=O bond lengths exists.

A recent paper by Kwon et al. [33], described the combination of cryo-trapping of Compound II species within larger crystals of two different peroxidases, that were then used for SF-ROX carried out at an unusually high X-ray energy of 15.2 keV allowing for very high-resolution data to be obtained. The structure of the Compound II intermediate in CcP was determined to 1.06 Å resolution, with two major benefits: firstly, at this resolution electron density is able to indicate likely positions of protons and identify protonation states of active site residues (Figure 2b) and secondly, estimation of bond length errors following unrestrained refinement in SHELXL [34]. The importance of this latter advantage is that the significance of bond length changes in structures between different states of an enzyme or indeed different enzymes may be assessed with a genuine assessment of coordinate error [33]. The data reported by Kwon et al. [33] complement the SFX study with DtpB [29], in that further support for variation in Fe(IV)=O bond lengths between species, and Compound I and II in peroxidases appear to exist (Figure 2c).

Time-resolved approaches to determining structures of defined intermediate states

Time-resolved SFX (Tr-SFX) is an emerging technique enabling enzyme reactions to be structurally characterised. The field has been excellently reviewed [35,36] recently and we provide specific examples here relevant to the study of Fe enzymes.

A comprehensive recent study on the fungal denitrification enzyme, cytochrome P450 nitric oxide reductase (P450nor) from *Fusarium oxysporum* highlighted the importance of complementary spectroscopy and molecular simulations to capture and reveal the nature of an intermediate species [17]. P450nor belongs to the cytochrome P450 superfamily (proximal Cys-heme ligation), but functions to reduce nitric oxide (NO) to form nitrous oxide (N_2O) via several intermediate species, rather than the canonical monooxygenase activity associated with P450s [37]. Following a previous Tr-SFX study that determined the structure of an initial Fe(III)–NO intermediate [38], Nomura et al. [17] sought to characterise a short-lived second intermediate

Figure 2

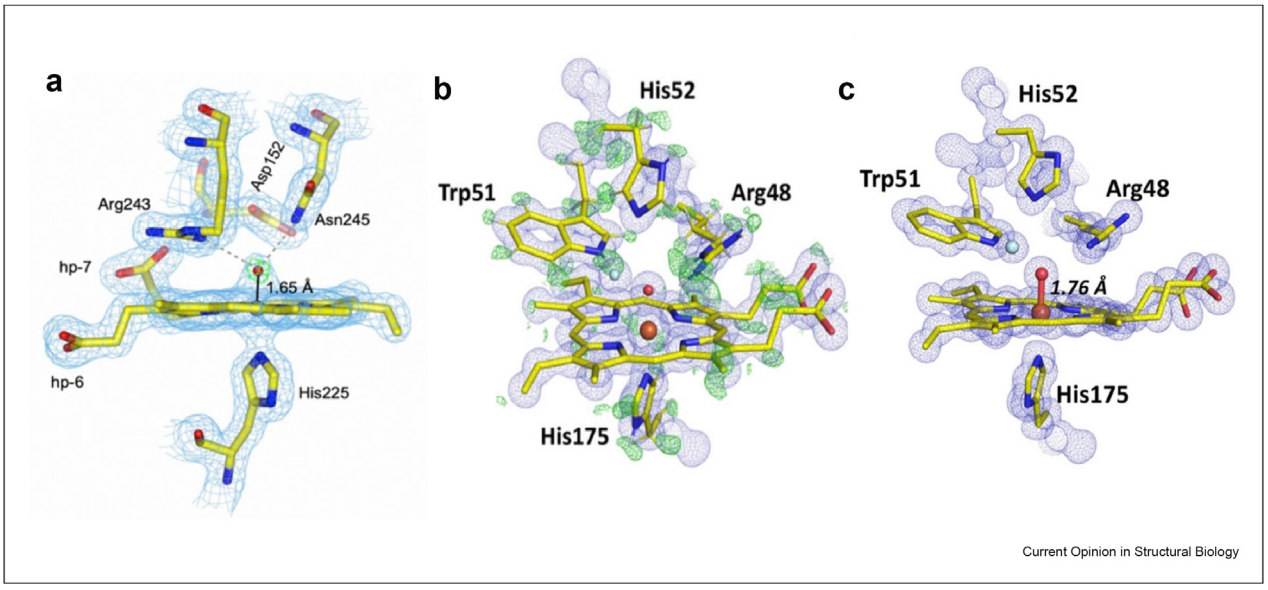

XFEL structures of heme peroxidases. **(a)** Room temperature 1.75 Å SFX structure of Compound I DtpB revealing a Fe−O bond length consistent with a Fe(IV)═O species (taken from Ref. [29]). Hp-6 and hp-7 refer to the propionate groups 6 and 7 respectively. (**b** and **c**) Cryo-cooled SF-ROX structures of yeast CcP Compound II (taken from Ref. [33]) **(b)** Difference map, revealing the positions of protons near to the active site, made possible due to the exceptionally high resolution (1.06 Å). **(c)** Ultrahigh-resolution structure revealed a Fe−O bond length of 1.76 Å consistent with a Fe(IV)═O species. In a peroxidase, the oxo intermediates, Compound I and II, undergo sequential one-electron reduction back to the ferric state, with concomitant one-electron oxidation of an organic substrate, or in the case of CcP, cytochrome *c*.

(***I***), activated by hydride transfer to the heme-bound NO from the electron donor NADH.

Thorough time-resolved solution spectroscopic studies identified the formation of intermediate ***I*** and investigated its lifetime in solution [17]. Crucially, reaction kinetics were then determined within populations of enzyme microcrystals using time-resolved visible spectroscopy (Figure 3a), revealing the formation of the intermediate 1 s after photolysis of caged NO, compared to 10 ms in solution [17]. The slower enzyme kinetics are attributed to crystal packing partially obscuring the substrate access channel for NADH [17]. Based on the spectroscopic data, the reaction within individual microcrystals was activated by light in the presence of NADH and the reaction arrested by cryo-cooling after 5 s. The resulting structure revealed a different heme-NO geometry in ***I*** *vs* the Fe(III)−NO intermediate determined by Tr-SFX (Figure 3b) [17]. Finally, the electronic structure of ***I*** was investigated by quantum mechanical/molecular mechanical simulations (QM/MM) to reveal that the crystal structure corresponded to a Fe(III)−$NHO^{\bullet-}$ species [17]. In terms of the P450nor catalytic mechanism, the identification of a singly protonated radical species demonstrates how N−N bond formation can be achieved through a radical−radical coupling mechanism with a second NO [17].

The preceding discussion relates to how structures of stable intermediate Fe species may be captured by room temperature static SFX, and certain intermediates may be cryo-trapped within either large single crystals or microcrystal populations for data collection at 100 K. A more general approach that allows entire reactions to play out within crystals, with multiple time points structurally characterised, has been described as a grand challenge in structural biology. This would allow us to move towards a fully dynamic depiction of enzyme catalysis under close to physiological conditions. Reactions may be initiated either by light (typically a laser with suitable excitation wavelength) [39] for either naturally photo-activated systems or using a photocage [40]. Alternatively, and more generally, reactions may be initiated by mixing microcrystals with substrates and other reagents. The scope of reaction initiation methods and mixing is beyond the scope of this article but in brief, mixing may be achieved by drop-on-drop approaches using fixed targets [41] or tape drive systems [14], microfluidics [42] or mix and inject technologies [43].

A tour-de-force in the use of Tr-SFX in partnership with XES is provided by Rabe et al. [44] who characterised the reaction of the non-heme Fe enzyme isopenicillin *N* synthase (IPNS) with ACV and O_2 to produce isopenicillin *N*, the precursor of all natural cephalosporins and

Figure 3

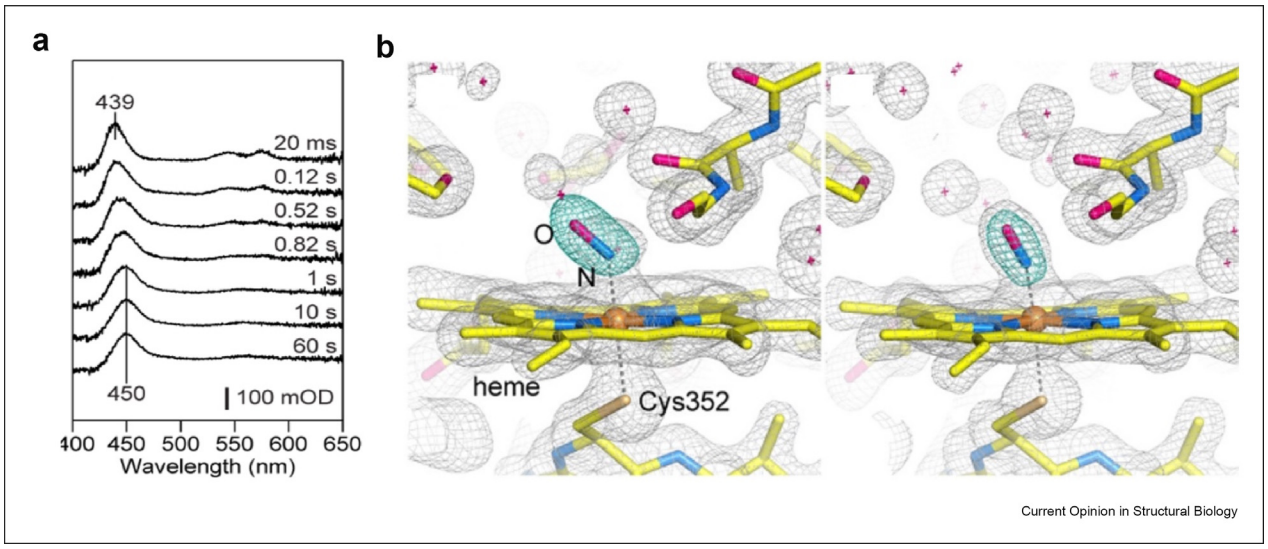

Cryo-trapped intermediate species in P450nor. **(a)** Time-resolved visible absorbance difference spectrum of P450nor microcrystals after caged NO photolysis. The difference absorbance peak maximum at 439 nm corresponds to the initial Fe(III)−NO complex and the peak maxima at 450 nm present after 1 s is the intermediate ***I***. **(b)** The cryo-trapped 1.8 Å SFX structure of ***I*** (left panel) and the SF-ROX structure of Fe(III)−NO (right panel [38]) corresponding to the difference spectrum peak maximum at 439 nm in **(a)**. In ***I*** the bound NO is significantly more bent (Fe−N−O = 138° compared to 158° in the Fe(III)−NO state; right panel), offering direct structural evidence for an Fe(III)−$NHO^{\bullet-}$ species, accounting for a mechanism of radical coupling with a second NO molecule to form N_2O. Images taken from Ref. [17].

penicillins. In this approach, microcrystals contained within droplets on a tape drive sample delivery system under anaerobic conditions were passed through an O_2 saturated chamber to initiate reactivity at room temperature. SFX and XES data were measured from the same XFEL pulses at time points between 400 and 3000 ms capturing the formation of an Fe(III) superoxide state (Figures 1b and 4) [44]. Crucially, the XES data allowed the oxidation states of the Fe atom of the active site to be explicitly identified at each time point (Figure 4a and b). Formation of the intermediate led to conformational changes throughout the enzyme, evidenced by atomic movements and changes in B-factors. XES data revealed changes consistent with the

Figure 4

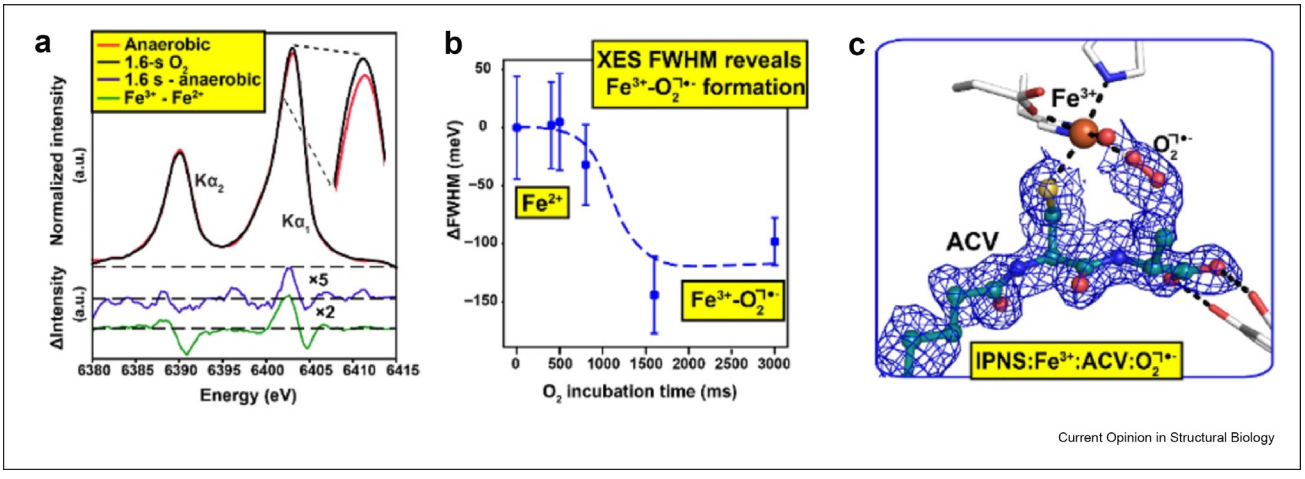

Combined Tr-SFX and XES study of IPNS. The reaction was initiated within crystals by exposure to O_2, with XES (**a** and **b**) used to monitor the subsequent reaction steps via the oxidation states of the Fe atom from Fe(II) to Fe(III). Electron density is shown in **(c)** for the superoxide intermediate (Fe(III)−$O_2^{\bullet-}$) identified at a 1600 ms time point, that abstracts the C-3 hydrogen from the ACV L-Cys (substrate) to form a thioaldehyde, which then undergoes 4-*exo*-tricyclization to produce a β-lactam ring linked via a S to the resulting Fe(IV)=O species [44].

formation of a Fe(III)-superoxide intermediate essential for the formation of the β-lactam ring through initiating a proton abstraction step (Figure 4c). The study provides significant insights into the role of protein dynamics in catalysis within Fe enzymes [44].

Remaining challenges and future opportunities

Several of the examples described in this article have highlighted the power of spectroscopic measurements from crystals to identify the electronic (redox) state of Fe-containing enzymes. However, a limitation arises when considering enzymes that contain multiple Fe atoms or several different types of Fe centre. Spectroscopic methods measure the average spectrum from all such chromophores. Sauter et al. [45] described a possible application of the spatially resolved anomalous dispersion (SPREAD) methodology originally applied by Einsle et al. [46] to SFX data. In its previous application, a series of monochromatic datasets are measured at intervals across an absorption edge allowing the X-ray absorption spectrum for each individual metal centre to be reconstructed. In principle, an alternative is to use the non-monochromatic nature of an XFEL (or suitable synchrotron) beam to collect data for these different wavelengths within a single pulse close to an absorption edge and thus reconstruct the oxidation states of individual metal centres such as those containing iron. Analysis of simulated data from a ferredoxin suggested that this may in principle be possible but requires substantial further development in methodology [45]. Should this be achieved, the resulting payoff in terms of understanding electronic states in multi-Fe systems would be considerable.

Identification of protonation states remains challenging within crystal structures although the use of NX can explicitly identify these, while increasingly powerful QM/MM simulation based on experimental structures can identify plausible combinations of active site residue electronic and protonation states and in turn can be used to guide interpretation of electron density for example of intermediate states [47]. Recent developments in the field highlight the challenges of working with Fe enzymes using serial methods, particularly those with higher valence electronic states. The availability of more complementary methods to measure spectroscopic data from crystals and to conduct computational simulations of the resulting structures are required.

Summary

SFX and complementary approaches are now available to allow for high-quality structure determination of Fe enzymes in both stable and time-resolved intermediate states. Spectroscopic or computational validation to assign structures to reaction steps remains very important for confidence in assigning catalytic mechanism. We anticipate that the next few years will see both the implementation of new reaction initiation and spectroscopic tools but also help to lower the barrier for new groups and projects into time-resolved structural enzymology, and so greatly increase the number of iron enzyme reactions studied in this manner.

Conflict of interest statement

Nothing declared.

Data availability

No data was used for the research described in the article.

Acknowledgements

The authors acknowledge funding from the BBSRC (BB/W001950/1; BB/R021015/1, BB/\01577X/1) supporting work on Fe-containing enzymes and work at XFEL and synchrotron sources, together with our many colleagues involved in SFX work.

References

1. Kendrew JC, Bodo G, Dintzis HM, Parrish RG, Wyckoff H, Phillips DC: **A three-dimensional model of the myoglobin molecule obtained by x-ray analysis**. *Nature* 1958, **181**: 662–666.

2. Perutz MF, Rossmann MG, Cullis AF, Muirhead H, Will G, North AC: **Structure of haemoglobin: a three-dimensional Fourier synthesis at 5.5-A. resolution, obtained by X-ray analysis**. *Nature* 1960, **185**:416–422.

3. Solomon EI, Goudarzi S, Sutherlin KD: **O2 activation by non-heme iron enzymes**. *Biochemistry* 2016, **55**:6363–6374.

4. Huang X, Groves JT: **Oxygen activation and radical transformations in heme proteins and metalloporphyrins**. *Chem Rev* 2018, **118**:2491–2553.

5. Jasniewski AJ, Que L: **Dioxygen activation by nonheme diiron enzymes: diverse dioxygen adducts, high-valent intermediates, and related model complexes**. *Chem Rev* 2018, **118**:2554–2592.

6. * Pfanzagl V, Beale JH, Michlits H, Schmidt D, Gabler T, Obinger C, Djinović-Carugo K, Hofbauer S: **X-ray-induced photoreduction of heme metal centers rapidly induces active-site perturbations in a protein-independent manner**. *J Biol Chem* 2020, **295**: 13488–13501.
A thorough characterisation of photoreduction of heme in crystals as a function of absorbed x-ray dose

7. Kekilli D, Moreno-Chicano T, Chaplin AK, Horrell S, Dworkowski FSN, Worrall JAR, Strange RW, Hough MA: **Photoreduction and validation of haem-ligand intermediate states in protein crystals by in situ single-crystal spectroscopy and diffraction**. *IUCrJ* 2017, **4**:263–270.

8. Shelley KL, Garman EF: **Quantifying and comparing radiation damage in the protein data bank**. *Nat Commun* 2022, **13**:1314.

9. Aller P, Orville AM: **Dynamic structural biology experiments at XFEL or synchrotron sources**. In *Structural Proteomics: High-Throughput Methods*. Edited by Owens RJ, Springer US; 2021:203–228, https://doi.org/10.1007/978-1-0716-1406-8_11.

10. Hough MA, Owen RL: **Serial synchrotron and XFEL crystallography for studies of metalloprotein catalysis**. *Curr Opin Struct Biol* 2021, **71**:232–238.

11. Wilson MA: **Mapping enzyme landscapes by time-resolved crystallography with synchrotron and X-ray free electron laser light**. *Annu Rev Biophys* 2022, **51**:79–98.

12. Grunbein ML, Nass Kovacs G: **Sample delivery for serial crystallography at free-electron lasers and synchrotrons**. *Acta Crystallogr D* 2019, **75**:178–191.

13. Nam KH: **Serial X-ray crystallography**. *Crystals* 2022, **12**:99.

14. * Butryn A, Simon PS, Aller P, Hinchliffe P, Massad RN, Leen G, Tooke CL, Bogacz I, Kim I-S, Bhowmick A, *et al.*: **An on-demand, drop-on-drop method for studying enzyme catalysis by serial crystallography**. *Nat Commun* 2021, **12**:4461.
This paper describes an exciting new method for drop-on-drop mixing of reagents with microcrystals on a tape drive system, compatible with XES and laser activation methods approaches

15. Hirata K, Shinzawa-Itoh K, Yano N, Takemura S, Kato K, Hatanaka M, Muramoto K, Kawahara T, Tsukihara T, Yamashita E, *et al.*: **Determination of damage-free crystal structure of an X-ray–sensitive protein using an XFEL**. *Nat Methods* 2014, **11**:734–736.

16. Suga M, Akita F, Yamashita K, Nakajima Y, Ueno G, Li H, Yamane T, Hirata K, Umena Y, Yonekura S, *et al.*: **An oxyl/oxo mechanism for oxygen-oxygen coupling in PSII revealed by an x-ray free-electron laser**. *Science* 2019, **366**:334–338.

17. ** Nomura T, Kimura T, Kanematsu Y, Yamada D, Yamashita K, Hirata K, Ueno G, Murakami H, Hisano T, Yamagiwa R, *et al.*: **Short-lived intermediate in N(2)O generation by P450 NO reductase captured by time-resolved IR spectroscopy and XFEL crystallography**. *Proc Natl Acad Sci U S A* 2021:118.
This paper describes a very thorough study to characterise the reactivity of an iron enzyme in solution and crystals using time-resolved visible and infrared spectroscopy. The time point identified was then used to cryo-trap a previously uncharacterised intermediate in the reaction mechanism for diffraction SFX data collection at 100 K on a mesh support

18. Halsted TP, Yamashita K, Hirata K, Ago H, Ueno G, Tosha T, Eady RR, Antonyuk SV, Yamamoto M, Hasnain SS: **An unprecedented dioxygen species revealed by serial femtosecond rotation crystallography in copper nitrite reductase**. *IUCrJ* 2018, **5**:22–31.

19. Shimada A, Kubo M, Baba S, Yamashita K, Hirata K, Ueno G, Nomura T, Kimura T, Shinzawa-Itoh K, Baba J, *et al.*: **A nanosecond time-resolved XFEL analysis of structural changes associated with CO release from cytochrome c oxidase**. *Sci Adv* 2017, **3**, e1603042.

20. Schroder GC, Meilleur F: **Metalloprotein catalysis: structural and mechanistic insights into oxidoreductases from neutron protein crystallography**. *Acta Crystallogr D* 2021, **77**:1251–1269.

21. Kwon H, Langan PS, Coates L, Raven EL, Moody PCE: **The rise of neutron cryo-crystallography**. *Acta Crystallogr D* 2018, **74**:792–799.

22. Lučić M, Wilson MT, Svistunenko DA, Owen RL, Hough MA, Worrall JAR: **Aspartate or arginine? Validated redox state X-ray structures elucidate mechanistic subtleties of Fe(IV) = O formation in bacterial dye-decolorizing peroxidases**. *J Biol Inorg Chem* 2021, **26**:743–761.

23. * Srinivas V, Banerjee R, Lebrette H, Jones JC, Aurelius O, Kim I-S, Pham CC, Gul S, Sutherlin KD, Bhowmick A, *et al.*: **High-resolution XFEL structure of the soluble methane monooxygenase hydroxylase complex with its regulatory component at ambient temperature in two oxidation states**. *J Am Chem Soc* 2020, **142**:14249–14266.
A detailed mechanistic study of soluble methane oxygenase in two different oxidation states of the diiron active site, with SFX combined with XES to confirm the oxidation state associated with each structure

24. Banerjee R, Jones JC, Lipscomb JD: **Soluble methane monooxygenase**. *Annu Rev Biochem* 2019, **88**:409–431.

25. Moody PCE, Raven EL: **The nature and reactivity of ferryl heme in compounds I and II**. *Acc Chem Res* 2018, **51**:427–435.

26. Berglund GI, Carlsson GH, Smith AT, Szoke H, Henriksen A, Hajdu J: **The catalytic pathway of horseradish peroxidase at high resolution**. *Nature* 2002, **417**:463–468.

27. Meharenna YT, Doukov T, Li H, Soltis SM, Poulos TL: **Crystallographic and single-crystal spectral analysis of the peroxidase ferryl intermediate**. *Biochemistry* 2010, **49**:2984–2986.

28. Gumiero A, Metcalfe CL, Pearson AR, Raven EL, Moody PC: **Nature of the ferryl heme in compounds I and II**. *J Biol Chem* 2011, **286**:1260–1268.

29. ** Lučić M, Svistunenko DA, Wilson MT, Chaplin AK, Davy B, Ebrahim A, Axford D, Tosha T, Sugimoto H, Owada S, *et al.*: **Serial femtosecond zero dose crystallography captures a water-free distal heme site in a dye-decolorising peroxidase to reveal a catalytic role for an arginine in Fe(IV) =O formation**. *Angew Chem Int Ed Engl* 2020, **59**:21656–21662.
This paper describes the structures of a heme peroxidase at cryogenic and room temperatures in the resting state ferric and unusually long-lived Compound I Fe(IV) intermediate states. Fixed target SFX was used to obtain intact RT structures of these radiation sensitive states, while spectroscopically validated multicrystal datasets at 100 K demonstrated that these were essentially identical to the SFX structures

30. Kwon H, Schrader TE, Ostermann A, Blakeley MP, Raven EL, Moody PCE: **Heme peroxidase-Trapping intermediates by cryo neutron crystallography**. *Methods Enzymol* 2020, **634**:379–389.

31. Chreifi G, Baxter EL, Doukov T, Cohen AE, McPhillips SE, Song J, Meharenna YT, Soltis SM, Poulos TL: **Crystal structure of the pristine peroxidase ferryl center and its relevance to proton-coupled electron transfer**. *Proc Natl Acad Sci U S A* 2016, **113**:1226–1231.

32. Shrestha R, Chen X, Ramyar KX, Hayati Z, Carlson EA, Bossmann SH, Song L, Geisbrecht BV, Li P: **Identification of surface-exposed protein radicals and A substrate oxidation site in A-class dye-decolorizing peroxidase from thermomonospora curvata**. *ACS Catal* 2016, **6**:8036–8047.

33. ** Kwon H, Basran J, Pathak C, Hussain M, Freeman SL, Fielding AJ, Bailey AJ, Stefanou N, Sparkes HA, Tosha T, *et al.*: **XFEL crystal structures of peroxidase Compound II**. *Angew Chem Int Ed Engl* 2021, **60**:14578–14585.
Kwon et al. describe extremely high-resolution SF-ROX structures that allow the modelling of hydrogen atoms in the electron density maps in order to answer long-standing questions about protonation states in heme peroxidases

34. Sheldrick G: **Crystal structure refinement with SHELXL**. *Acta Crystallogr C* 2015, **71**:3–8.

35. * Orville AM: **Recent results in time resolved serial femtosecond crystallography at XFELs**. *Curr Opin Struct Biol* 2020, **65**:193–208.
A thorough and clear review of the current state-of-the-art in time resolved XFEL serial crystallography

36. Malla TN, Schmidt M: **Transient state measurements on proteins by time-resolved crystallography**. *Curr Opin Struct Biol* 2022, **74**, 102376.

37. Su F, Takaya N, Shoun H: **Nitrous oxide-forming codenitrification catalyzed by cytochrome P450nor**. *Biosci, Biotechnol, Biochem* 2004, **68**:473–475.

38. Tosha T, Nomura T, Nishida T, Saeki N, Okubayashi K, Yamagiwa R, Sugahara M, Nakane T, Yamashita K, Hirata K, *et al.*: **Capturing an initial intermediate during the P450nor enzymatic reaction using time-resolved XFEL crystallography and caged-substrate**. *Nat Commun* 2017, **8**:1585.

39. Grünbein ML, Stricker M, Nass Kovacs G, Kloos M, Doak RB, Shoeman RL, Reinstein J, Lecler S, Haacke S, Schlichting I: **Illumination guidelines for ultrafast pump-probe experiments by serial femtosecond crystallography**. *Nat Methods* 2020, **17**:681–684.

40. Monteiro DCF, Amoah E, Rogers C, Pearson AR: **Using photocaging for fast time-resolved structural biology studies**. *Acta Crystallogr D* 2021, **77**:1218–1232.

41. Mehrabi P, Schulz EC, Agthe M, Horrell S, Bourenkov G, von Stetten D, Leimkohl J-P, Schikora H, Schneider TR, Pearson AR, *et al.*: **Liquid application method for time-resolved analyses by serial synchrotron crystallography**. *Nat Methods* 2019, **16**:979–982.

42. Calvey GD, Katz AM, Pollack L: **Microfluidic mixing injector holder enables routine structural enzymology measurements**

with mix-and-inject serial crystallography using X-ray free electron lasers. *Anal Chem* 2019, **91**:7139–7144.

43. Pandey S, Calvey G, Katz AM, Malla TN, Koua FHM, Martin-Garcia JM, Poudyal I, Yang J-H, Vakili M, Yefanov O, *et al.*: **Observation of substrate diffusion and ligand binding in enzyme crystals using high-repetition-rate mix-and-inject serial crystallography**. *IUCrJ* 2021, **8**:878–895.

44. ** Rabe P, Kamps J, Sutherlin KD, Linyard JDS, Aller P, Pham CC, Makita H, Clifton I, McDonough MA, Leissing TM, *et al.*: **X-ray free-electron laser studies reveal correlated motion during isopenicillin N synthase catalysis**. *Sci Adv* 2021, **7**.

This paper provides a very clear example of the combination of multi-time point Tr-SFX under carefully controlled experimental conditions with XES spectroscopy to follow the redox state of the Fe and hence to identify a novel superoxide intermediate in the IPNS reaction pathway

45. * Sauter NK, Kern J, Yano J, Holton JM: **Towards the spatial resolution of metalloprotein charge states by detailed modeling of XFEL crystallographic diffraction**. *Acta Crystallogr D* 2020, **76**:176–192.

A fascinating proof of concept study describing application of the spatially resolved anomalous dispersion method to SFX data, potentially allowing the redox states of individual iron atoms in a structure to be resolved

46. Einsle O, Andrade SLA, Dobbek H, Meyer J, Rees DC: **Assignment of individual metal redox states in a metalloprotein by crystallographic refinement at multiple X-ray wavelengths**. *J Am Chem Soc* 2007, **129**:2210–2211.

47. Sen K, Hough MA, Strange RW, Yong C, Keal TW: **QM/MM simulations of protein crystal reactivity guided by MSOX crystallography: a copper nitrite reductase case study**. *J Phys Chem B* 2021, **125**:9102–9114.

48. Elango N, Radhakrishnan R, Froland WA, Wallar BJ, Earhart CA, Lipscomb JD, Ohlendorf DH: **Crystal structure of the hydroxylase component of methane monooxygenase from Methylosinus trichosporium OB3b**. *Protein Sci* 1997, **6**:556–568.

49. Pullin J, Wilson MT, Clémancey M, Blondin G, Bradley JM, Moore GR, Le Brun NE, Lučić M, Worrall JAR, Svistunenko DA: **Iron oxidation in Escherichia coli bacterioferritin ferroxidase centre, a site designed to react rapidly with H(2) O(2) but slowly with O(2)**. *Angew Chem Int Ed Engl* 2021, **60**:8361–8369.

50. Dickerson JL, McCubbin PT, Garman EF: **F. RADDOSE-XFEL: femtosecond time-resolved dose estimates for macromolecular X-ray free-electron laser experiments**. *J Appl Crystallogr* 2020, **53**:549–560.